EASR

Engineering and Applied Science Research

https://www.tci-thaijo.org/index.php/easr/index

Published by the Faculty of Engineering, Khon Kaen University, Thailand

Design and fabrication of a downdraft gasifier coupled with a small-scale diesel engine

Monorom Rith*[1)], Bernard Buenconsejo[2)] and Jose Bienvenido M. Biona[1)]

[1)]Department of Mechanical Engineering, De La Salle University, 2401 Taft Ave, Manila City, Metro Manila, Philippines
[2)]Department of Total Sensing Solutions, Keyence Philippines Inc., 6789 Ayala Avenue, Makati City, Metro Manila, Philippines

Received 4 August 2019
Revised 28 September 2019
Accepted 22 October 2019

Abstract

Gasification technology plays a significant role to increase the potential exploitation of agro-waste products. This technology can convert solid dried biomass into a combustible gas, widely called syngas or producer gas. Producer gas can be used to run a diesel engine in a dual fuel mode to partially reduce diesel fuel consumption. However, determination of the dimensions of a gasifier and gas cleaning elements for a pre-specified capacity of a pilot-scale diesel engine remains unexplored. This study, therefore, intends to provide a heuristic concept to avoid an oversize, cumbersome design of a gasifier and a gas cleaning unit based on basic theory. A 5.7 kW diesel engine and a Jatropha seed feedstock were selected for our study. A type of closed top, throatless, downdraft gasifier with an annular space was chosen. A cyclone filter, a shell-tube heat exchanger, and a dried-bed filter were selected as the components of the gas cleaning unit. The cyclone filter's dimensions were determined using the ideal gas principle. Next, basic heat transfer theory and fluid dynamics were applied to design a shell-tube heat exchanger. The results highlighted that the inner diameter of the designed gasifier should be 150 mm, and gasifier produced up to 27 kg/h of gas. At a biomass consumption rate of 5 kg/h, the gas production rate was 20 kg/h that substituted the diesel fuel consumption rate by up to 49% at 70% of the fuel engine load. It is noteworthy that the gasification efficiency of Jatropha seed was 77%. The proposed concept is expected to be informative for the design of other gasifier types suitable for different biomass types. This technical article is written in a simple way, which is very useful for practitioners to understand and apply it for the fabrication of a small-scale gasifier-engine system.

Keywords: Gasifier, Diesel engine, Jatropha seed, Producer gas, Product design

1. Introduction

Overuse and misuse of fossil fuel in recent years has triggered an increase in oil prices and reservoir depletion. Biomass-to-bioenergy conversion is considered a renewable technology that can mitigate fossil fuel dependency. It can be explained that biomass is produced in a short time, and this technology has a minor negative impact on the environment. Also, the technology can reduce imported fossil fuel consumption and minimize exhaust gas emissions into the atmosphere [1]. Bioenergy production can be by either a biological or chemical route.

Gasification technology is a thermo-chemical process that can convert a carbonaceous material into a combustible gas, called syngas or producer gas [2]. Producer gas can be used to run a spark ignition (SI) engine to fully replace gasoline [3-4] and a compression ignition (CI) engine to partially replace diesel fuel [5-6]. This technology has received increasing interest for electricity generation in remote rural areas for decentralized power generation when there is difficulty in accessing fossil fuels [7]. Producer gas was widely used to run diesel engines in a dual fuel mode rather than the SI engines on a neat gas mode in view of a lower power derating and minor engine modifications required [8]. The diesel replacement rate was 86% when the dual-fuel engine was operated at the maximum diesel replacement rate and 60% of the full engine load [9].

Gasification reactors consist of various specific designs based on their end-use purpose, energy output capacity, biomass type, conversion medium and gas quality [10]. For a gasifier coupled with a small-scale diesel engine, a downdraft gasifier is generally used because it can produce cleaner gas compared to other designs. It is intuitive that the fabrication costs of the cleaning system are less than those of other designs. The integrated downdraft gasifier-diesel engine system has been extensively used to study the technical feasibility, emissions, and combustion characteristics of a producer gas-diesel dual fuel mode by [5, 11-14]. Hydrogen can possibly be added to the producer gas to improve engine performance [15-16]. Biodiesel fuel can also be used to run a diesel engine with producer gas to replace even more diesel fuel [8, 17].

*Corresponding author. Tel.: +63 966 480 9818
Email address: rith_monorom@dlsu.edu.ph

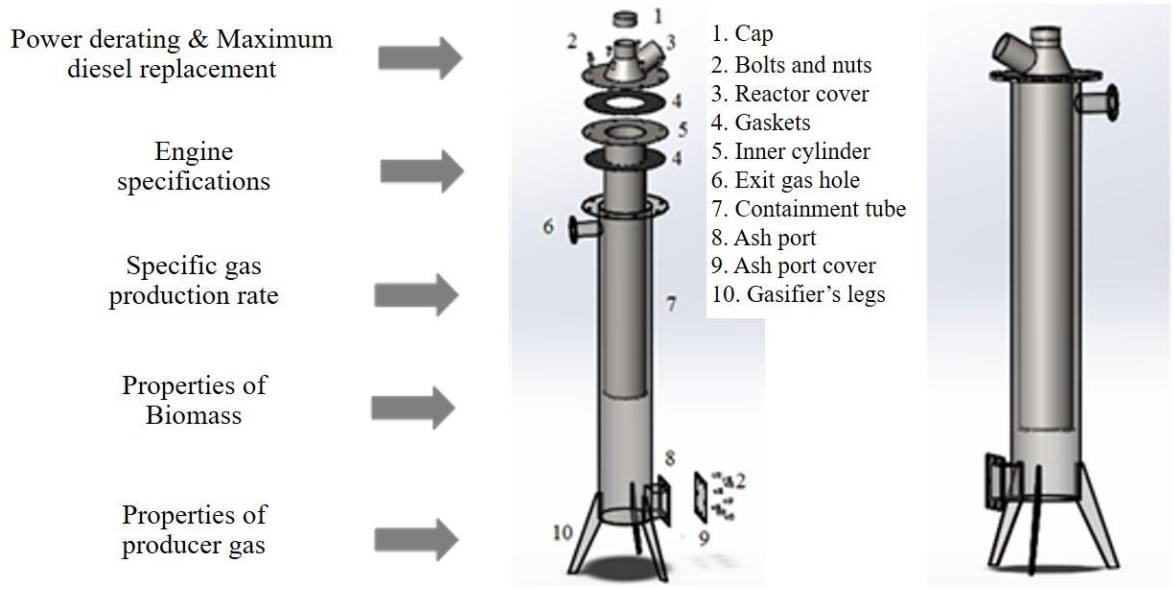

Figure 1 Closed-top, Throatless, Downdraft Gasifier

To the best of our knowledge, no study has proposed a heuristic concept to determine the dimensions of a gasifier and its gas cleaning components considering basic theory for a pilot-scale diesel engine. The gas at the gasifier exit is very hot and dirty. The product gas is laden with fly ash, particulate matter, and bio-oil (tar content). These undesired substances cause excessive wear to the main components of the engine, i.e., piston head, piston rings, cylinders, and valves. Such substances, additionally, affect the long term reliability of an engine.

Correspondingly, this present study intends to provide a heuristic concept to design a downdraft gasifier and its cleaning system based on the basic theory of fluid dynamics and heat transfer to avoid an oversize and cumbersome design. A KM 186F diesel engine with a capacity of 5.7 kW and a Jatropha seed feedstock were selected for use in a gasifier system. The designed gasifier system was sequentially fabricated and coupled with the engine for the experiment. The proposed design concept is expected to produce an efficiently designed gasifier and gas cleaning unit, reduce fabrication costs, improve gasification efficiency, and reduce engine maintenance costs. This heuristic concept is also expected to be applicable to the design of further gasifier types for other kinds of biomass and fuel.

The remainder of the article is structured as follows. Section 2 covers the specific gasifier design. Section 3 provides calculations for design of the gas cleaning unit, while Section 4 describes fabrication of the gasifier system coupled to an engine. Then in Section 5, the observed results, engine performance and emission characteristics are discussed. Finally, Section 6 offers concluding thoughts and recommendations.

2. Specific gasifier design

2.1 Closed-top, throatless, downdraft gasifier

A co-current gas producer unit (sometimes called a downdraft gasifier) is often used with a diesel engine to run on dual fuel mode because it is the most appropriate for pilot scale. This kind of gasifier has various designs. In this study, a closed-top, throatless gasifier with an annular space is selected to study. The gasifier is cylindrical in shape, comprised of two concentric cylinders. This gasifier is suitable for a small-scale diesel engine and the fabrication costs are relatively low. Furthermore, a downdraft gasifier produces the gas with a lower tar content compared with an updraft gasifier [10]. Tar is the primary concern of gasification because production of this constituent leads to engine failure. A lower content of tar in producer gas results in minimization of fabrication costs of the gas cleaning unit and operation costs of gas cleaning. Figure 1 illustrates the closed top, throatless, downdraft gasifier and the required parameters to identify the dimensions of the gasifier.

2.2 Dimensions of the downdraft gasifier

A KM 186F diesel engine was selected for this study. The fuel consumption for the engine at a speed of 3,000 rpm was 275.1 g/kWh [18]. This engine produced a brake power of up to 5.7 kW at 3,000 rpm [18]. Therefore, a total diesel consumption rate of 1.568 kg/h produced 5.7 kW. The calorific value of diesel fuel is typically 42 MJ/kg. Thus, the thermal energy supplied for 5.7 kW of power at 3,000 rpm was 65.856 MJ/h.

A higher amount of producer gas to replace the diesel fuel resulted in a power de-rating of about 20% [17]. The producer gas replaced up to 64% of the diesel fuel [19] or 71% of the diesel fuel [17]. In our study, the respective power de-rating and maximum diesel replacement were projected to be 20% and 65%, respectively. At a high engine load, the thermal brake efficiency of the neat diesel mode was about 22.5%, while the thermal brake efficiency of the dual-fuel mode was about 15% at the maximum diesel replacement rate [20]. Correspondingly, the total thermal energy consumption of the producer gas in place of the diesel fuel equaled 65.87 (MJ/h) × 80% × 65% × (22.5 % / 15 %) = 51.37 MJ/h.

The caloric value of producer gas ranges from 3.5 to 6.5 MJ/m^3 as reported in previous literature. A value of 4.24 MJ/m^3 or 3.88 MJ/kg was the mean of the calorific

Table 1 Mechanical and physical properties of 27 ℃ gases and 5 ℃ water [21]

Properties	CO	H_2	CO_2	CH_4	N_2	Producer gas	Water
Specific Heat C_p (J/kg K)	1,048	14,491	942	2,448	1,046	1,348.612	4,206 [b]
Absolute viscosity μ 10^{-6} (N s/m^2)	22.190	10.864	19.320	11.800	21.98	23.10885	1,535 [b]
Thermal conductivity k (w/m k)	0.032	0.228	0.025	0.037	0.03335	0.066339	0.568 [b]
Density ρ (kg/m^3)	1.139 [a]	0.08185 [a]	1.797 [a]	0.653 [a]	1.142 [a]	1.090 [a]	1 000 [b]

[a] at 27℃; [b] at 5℃

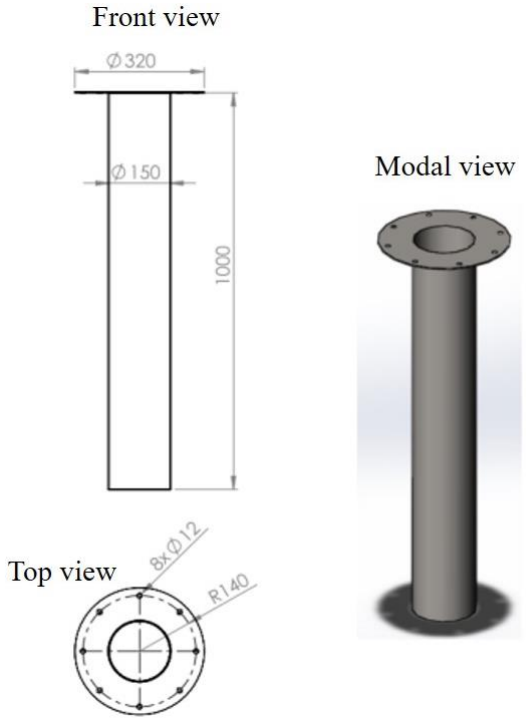

Figure 2 Mechanical CAD drawing of the inner cylinder

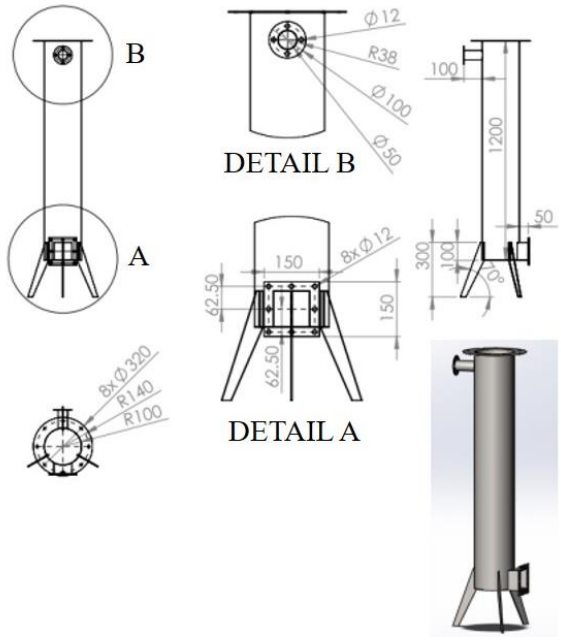

Figure 3 Mechanical CAD drawing of the outer cylinder

values given in previous studies. In our study, the calorific value of the gas was assumed to be 4.24 MJ/m^3 or 3.88 MJ/kg. The density of the gas is 1.09 kg/m^3 at 1 atm and 27 ℃ (see Table 1).

The producer gas flow rate was assumed to be $\frac{Thermal\ eneryg\ consumption\ rate\ of\ gaseous\ fuel\ (MJ/h)}{Calorific\ value\ of\ gaseous\ fuel\ (MJ/m^3)} = \frac{51.37}{4.24} = 12.14$ m^3/h at ambient temperature. Correspondingly, the amount of producer gas used to replace the diesel was found to be 13.24 kg/h or 12.14 m^3/h. The maximum gasification efficiency was determined to be 410 m^3/h.m^2 of the specific gas production rate (SGPR) [22]. The inside cross-sectional area of the reactor is the ratio of the volumetric velocity of the gas to the SGPR.

Therefore, the maximum cross-sectional area of the inner cylinder equals $\frac{12.14\ m^3/h}{410\ m^3/h.m^2} = 0.0296\ m^2$. In other words, the maximum diameter of the inside cylinder was 194 mm.

This reactor was designed to convert Jatropha seed into the gas, and the maximum size of the seeds was around 10 mm. The maximum particle size of the biomass was recommended as one-eighth of the inner cylinder diameter to avoid biomass bridging [23]. Therefore, the inner cylinder's diameter for the Jatropha seed feedstock should be larger than 80 mm and smaller than 194 mm. An appropriate diameter of the inner cylinder should be chosen to avoid biomass bridging and mitigate an oversized design. Eventually, a 150 mm inner cylinder diameter was chosen in our study to ensure that the biomass flow rate is smooth and constant, fabrication costs are minimized, and gasification efficiency is high.

The annular space (the space between the outer and inner cylinders) is proportional to the diameter of the outer cylinder. If the annular space increases, the amount of residence time and reaction time becomes longer, thereby improving the quality of the gas and gasification efficiency [22]. However, the fabrication costs are higher. The outer cylinder was designed to be 200 mm in diameter in our study. The gasification efficiency is in line with the reactor height. However, the cost of fabrication was increased. Eventually, the best height of the outer cylinder was determined to be 1,200 mm, whereas the height of the inner cylinder was 1,000 mm. Therefore, the length of the outer cylinder was 200 mm longer than the inner cylinder. The inner cylinder and the containment tube were made of black iron metal sheet with thicknesses of 3 mm and 1.5 mm, respectively. This gas producer was designed to operate in a batch mode. Mechanical CAD drawings of the inner and outer cylinders are illustrated in Figures 2 and 3, respectively. The fabrication costs of the reactor were 500 USD, including metal, labor, and an insulator. Rock wool was used to wrap the outer cylinder to reduce heat losses.

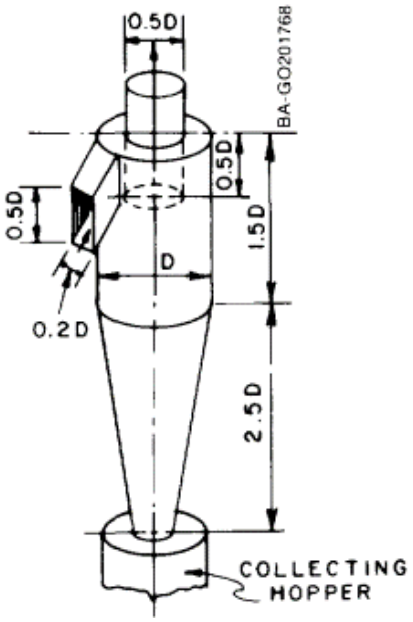

Figure 4 Cyclone separator dimensions [24]

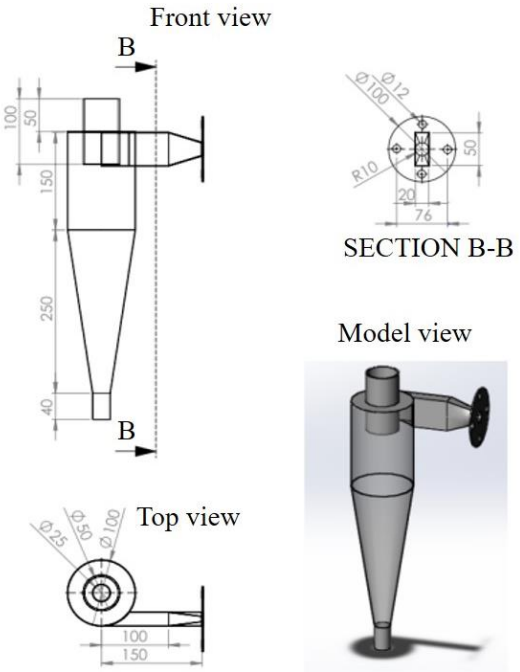

Figure 5 Mechanical CAD drawing of the cyclone filter

3. Cooling-cum-cleaning unit

3.1 Cyclone separator

A cyclone filter is usually used as a preliminary cleaner for gas producer because this kind of filter can collect high temperature dust and cool the gas. It is a gravitational separator that is primarily influenced by the inlet air velocity. Reed and Das recommended that the minimum gas velocity should be 15 m/s to collect medium-sized dust and 25 m/s to separate the heavy dust from the gas flow [24].

In the present study, the cyclone separator was designed as a pre-filter connected between the reactor and a heat exchanger. The hot gas velocity flowing inside the cyclone filter was assumed to be greater than 25 m/s. Based on the above calculation, a producer gas flow rate of 12.14 m^3/h or 202.58 L/min at 27 ℃ was used to replace the maximum diesel fuel consumption. The gas temperature at the gasifier exit was between 200 and 300 ℃ [23] or about 200 ℃ [25]. In our study, the exit gas temperature was assumed to be 250 ℃ as the hot gas moved out of the reactor near the top through the annular space (see Figure 1). Determination of the cyclone separator's dimensions was based on the principles presented by [24]. The dimensions are illustrated in Figure 4, where, D, refers to diameter. The inlet pipe's width at the cyclone filter should be equal to the gasifier outlet pipe diameter [24]. The maximum diameter of the gasifier exit is calculated as the following, based on the ideal gas principle:

$P_1V_1 = nRT_1$ For the cooled gas at the engine inlet.
$P_2V_2 = nRT_2$ For the hot gas at the gasifier outlet.

$$\frac{P_1V_1}{P_2V_2} = \frac{nRT_1}{nRT_2}$$

We supposed no pressure loss along the pipe: $P_1 = P_2$.

$$\frac{V_1}{V_2} = \frac{T_1}{T_2} \Leftrightarrow \frac{\dot{V}_1}{\dot{V}_2} = \frac{T_1}{T_2};$$

where $\dot{V}_1$ and $\dot{V}_2$ are the volumetric flow rates of the gas at the engine inlet and the gasifier outlet, respectively.

$$\dot{V}_2 = \dot{V}_1\frac{T_2}{T_1} = (202.58\ \text{L/min}) \times \frac{523\ \text{k}}{300\ \text{k}} = 353\ \text{L/min}$$

However, $\dot{V}_2 = A_2v_2 = \frac{\pi D^2}{4}v_2$; v_2 is the gas velocity (m/s) at the gasifier outlet and v_2 should be less than 25 m/s, as discussed above.

$$d < \sqrt{\frac{4\,\dot{V}_2}{\pi v_2}} = \sqrt{\frac{4\,(353\ \text{L/min})}{\pi(25\ \text{m/s})}} = 55\ \text{mm}$$

According to the theoretical results, the diameter of the inner cylinder should be less than 55 mm. If the diameter is smaller, the efficiency of dust removal is better and the fabrication costs are also lower. A diameter of 20 mm, therefore, was selected in our study. As discussed above, this kind of filter was placed after the reactor and before the heat exchanger. The cyclone separator was made of black iron metal sheet with a thickness of 1 mm. The mechanical CAD drawing of the cyclone filter is shown in Figure 5. The cyclone filter cost was 80 USD, including material and labor.

3.2 Shell-tube heat exchanger

Most of the previous studies used a water spray to capture the undesired constituents laden in the gas and to cool it. This technique is efficient and simple, but it is associated with the high costs of water purification prior to disposal. Use of a heat exchanger is another way to clean and cool gas. A heat exchanger, therefore, was chosen in our study to cool the gas and remove tar even though it is more expensive than a liquid bath and tower.

Table 2 Price list of ½' pipe in Manila City

Material	Black iron (BI)	Galvanized iron (GI)	Stainless steel (SS)	Brass	Copper
Price (USD)	6	9	14	19.72	24

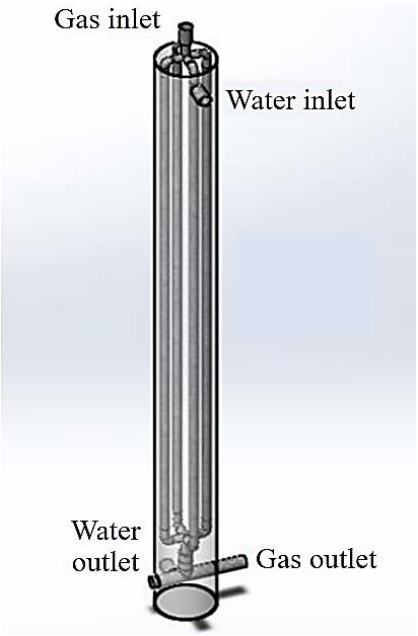

Figure 6 Modal view of the shell-tube heat exchanger

The dimensions of a shell-tube heat exchanger are calculated as follows.

3.2.1 Assumptions of the percentages of producer gas constituents

The gas composition and their fractions were assumed before design of the heat exchanger as follows. The producer gas is composed of CO, H_2, CO_2, CH_4, N_2, O_2, C_2H_2, and C_2H_6. The fractions of C_2H_2, C_2H_6, and O_2 are very marginal, based on published data of [23] and [26]. The percentages of these three gases were assumed to be zero. The proportions of the producer gas constituents are governed by the specific gasifier design, the operating parameters, the chemical-physical properties of biomass and time of operation [2, 10, 13]. We assumed that the producer gas was composed of CO = 17.50%, H_2 = 12.50%, CO_2 = 15%, CH_4 = 3%, and N_2 = 52%. The properties of the gases are listed in Table 1.

3.2.2 Flow characteristics of the producer gas and cooling water

Water at a constant temperature of 5 ℃ was used to cool the gas close to the ambient temperature, 27 ℃. The co-current flow concept was selected. In this design, the outside and inside diameters of the tube were 21.3 mm and 15.76 mm, respectively, whereas the inside diameter of the PVC black pipe was 155 mm. The gas flow rate was assumed to be 202.58 L/min or 3.68×10^{-3} kg/s, whereas the water flow rate was 10 L/min or 0.166 kg/s.

For gas:

$$\mathrm{Re} = \frac{4\dot{m}}{\mu\pi D_{in}} = \frac{4\times(3.68\times10^{-3}\ \mathrm{kg/s})}{(16.09\times10^{-6}\ \mathrm{N\ s/m^2})\times\pi\times(15.76\times10^{-3}\mathrm{m})} = 18.48\times10^{3}$$

For water:

$$\mathrm{Re} = \frac{4\dot{m}}{\mu\pi D} = \frac{4\times(0.166\ \mathrm{kg/s})}{(1{,}535\times10^{-6}\ \mathrm{N\ s/m^2})\times\pi\times(155\times10^{-3}\mathrm{m})} = 0.88\times10^{3}$$

The flow in a round pipe is laminar or turbulent if the Reynold number of the fluid is lower than 2,100 or higher than 4,000, respectively [27]. Therefore, the flow patterns of gas and water are laminar and turbulent, respectively.

3.2.3 Assumption of surface temperature

The rate of heat transfer is $\dot{q} = \dot{m}\ c_p\ \Delta T$. The rate of heat transfer of gas is equal to that of water.

For gas:

$$\dot{m}\ c_p = 3.68\times10^{-3}\ (\mathrm{kg/s})\times 1{,}348(\mathrm{J/kg\ K}) = 4.94\ \mathrm{W/K}$$

For water:

$$\dot{m}\ c_p = 0.166\ (\mathrm{kg/s})\times 4{,}206(\mathrm{J/kg\ K}) = 698.19\ \mathrm{W/K}$$

Based on the calculation above, the temperature of water at the exit slightly increases compared to the decrease of the gas temperature at the exit. In this study, the temperatures of the water at the inlet and outlet were assumed to be the same. Therefore, the outer surface temperature of the tube was assumed to be uniform.

3.2.4 Average heat transfer coefficient $\overline{h}_c$ (w/m²k)

Due to the turbulent flow of the gas and constant surface temperature, the Nusselt (Nu) number is 890 [28].

$$\mathrm{Nu} = \frac{\overline{h}_c D_{in}}{k} \Rightarrow \overline{h}_c = \frac{\mathrm{Nu}\ k_{gas}}{D_{in}}$$

where k_{gas} is the thermal conductivity of the producer gas.

For gas:

$$\left(\overline{h}_c\right)_{gas} = \frac{890\times(0.06634\ \mathrm{w/mk})}{(15.76\times10^{-3}\mathrm{m})} = 3{,}742\ \mathrm{w/m^2k}$$

3.2.5 Effect of thermal conductivity of the tubes on the heat transfer rate

A heat transfer rate is $\dot{q} = \mathrm{UA(LMTD)}$

where LMTD is the log mean temperature difference, U is the overall heat transfer coefficient (W/m².k), and A is the contact area (m²).

$$\mathrm{UA} = \frac{1}{\frac{1}{2\pi r_i L\left(\overline{h}_c\right)_{gas}} + \frac{1}{2\pi KL}\ln\left(\frac{r_o}{r_i}\right)}$$

$$= \frac{1}{\left[\frac{1}{2\pi\times(15.76\ \mathrm{mm})\times(6\mathrm{m})\times(3{,}742\ \mathrm{w/m^2k})}\right] + \left[\frac{1}{2\pi\times(\mathrm{k})\times(6\mathrm{m})}\ln\left(\frac{21.3\ \mathrm{mm}}{15.76\ \mathrm{mm}}\right)\right]}$$

Figure 7 Dried-bed filter

$$= \frac{1}{13{,}821 + \frac{7.99 \times 10^{-3}}{\mathrm{k}}} \ (\mathrm{W/K})$$

k is the thermal conductivity of the metal. The value of k is normally higher than 1 (W/m^2 K). Based on UA (W/K) above, the thermal conductivity, k, does not affect UA.

3.2.6 Choosing materials to make the shell-tube heat exchanger

Black PVC pipe with an inner diameter of 155 mm was chosen to make the shell because it cost only 14 USD for a pipe of 3 m in length. For the tube, five different materials were chosen for comparison, black iron (BI), galvanized iron (GI), stainless steel (SS), brass, and copper. These materials are commercially available. The specification of their diameter is the same, ½ in. The prices of these materials, listed in Table 2, are based on their retail prices in Manila City, the Philippines.

Copper and brass have a higher thermal conductivity compared to BI, GI, and SS. However, they are much more expensive. BI is the most inexpensive, but its resistance to corrosion is lower than that of GI.

Galvanized iron pipe was selected to make the tubes in this study due to a favorable tradeoff between its cost, 9 USD per pipe with a length of 6 m and high corrosion resistance.

3.2.7 Length of tube

As stated previously, the temperature of the gas at the reactor exit was assumed to be 250 ℃. Subsequently, we assumed that the gas temperature would drop to 100 ℃ after passing the cyclone separator. The tube-shell heat exchanger was designed to cool the producer gas from 100 ℃ to roughly 27 ℃ (the ambient temperature). Water at a temperature of 5 ℃ was chosen to flow across the shell, and this temperature was assumed to remain constant. The inner and outer diameters of the tube were 15.76 mm and 21.3 mm, respectively. The gas flow rate was assumed to be 3.68×10^{-3} kg/s. The length of the tube is calculated as follows:

- Heat transfer rate:

$$\dot{q}_c = \dot{m}\, c_p\, \Delta T = (3.68 \times 10^{-3}\ \mathrm{kg/s}) \times (1{,}348\ \mathrm{J/kg.K}) \times (60\ \mathrm{K}) = 297.64\ \mathrm{W}$$

However, $\dot{q}_c$ is equivalent to $\left(\overline{h}_c\right)_{gas} A\ (\mathrm{LMTD})$, according to [21].

- LMTD:

$$\mathrm{LMTD} = \frac{\Delta T_{out} - \Delta T_{in}}{\ln(\Delta T_{out}/\Delta T_{in})} = \frac{(100-5)-(27-5)}{\ln[(100-5)/(27-5)]} = 60.08\ \mathrm{K}$$

- Length of tube:

$$\left(\overline{h}_c\right)_{gas} A\ (\mathrm{LMTD}) = 297.64\ \mathrm{W}$$

The contact surface, A, is equal to $\pi D_i 4L$, and there are four tubes.

$$\overline{h}_c\ (\pi D_i 4L)(\mathrm{LMTD}) = 297.64\ \mathrm{W}$$

$$L = \frac{297.64}{4\pi D\left(\overline{h}_c\right)_{gas}\ \mathrm{LMTD}}$$

$$= \frac{297.64\ \mathrm{W}}{4 \times \pi \times (15.76 \times 10^{-3}\mathrm{m})(15.39\ \mathrm{W/m^2k}) \times (60.08\ \mathrm{K})}$$

$$= 1.62\ \mathrm{m}$$

Figure 8 Gasifier-generator unit (left), producer gas flame (upper right), and tar (lower right)

Table 3 Fabrication costs of the gasifier system

Gasifier system	Fabrication cost (USD)
Reactor	500
Cyclone filter	80
Shell-tube heat exchanger	59.28
Dried-bed filter	10
Total	649.28

1 USD = 50 PHP

Table 4 Basic technical specifications of the gasifier

Item	Description
Type	Closed-top, throatless, downdraft
Gasifier's weight (kg)	30
Critical dimension (mm)	D = 350 / h = 1800
Capacity (kW_{th})	130
Consumption rate (kg/h)	5
Biomass feedstock	Jatropha seed
Efficiency (%)	~77

Thus, the length of each tube is 1.62 m. The total length of four tubes is $1.62\ \text{m} \times 4 = 6.50\ \text{m}$. A ½–in GI pipe is 6 m in length. It was used to make the tubes for the shell-tube heat exchanger. In our study, we cut a 6 m GI pipe into four pieces, and therefore, each piece was 1.50 m in length. The model view of the shell-tube heat exchanger is illustrated in Figure 6. The total fabrication costs of the shell-tube heat exchanger were 59.28 USD (including labor, water pump, silicone gasket, and pipe fittings, adapters, and valves).

3.3 Dried-bed filter

The dried bed filter made of small-sized charcoal pieces and a synthetic fiber filter was designed for this study. This filter can absorb the remaining tar and filter small-sized particles. It was the last stage of the cooling-cum-cleaning unit, and it is installed after the heat exchanger. This filter costs 10 USD, i.e., 5 USD for the plastic tank, 2 USD for the charcoal particles layered below a synthetic fiber filter, and 3 USD for the synthetic fiber filter. Figure 7 presents photographic images of the dried-bed filter.

4. Fabrication of the gasifier system coupled to the engine

After the system was designed based on theory and empirical findings of the previous studies, the small-scale gasifier system was fabricated. The cost of each component is listed in Table 3. Figure 8 shows photographic images of the gasifier-generator system, the flame of the Jatropha seed-derived producer gas, and a jar of the resulting tar. A schematic diagram of this gasifier-engine system is shown in Figure 9. The system was comprised of a gasifier, cyclone filter, shell-tube heat exchanger, dried-bed filter, and diesel generator. The gasifier specifications are listed in Table 4.

Four k-type thermocouples were mounted at various positions to measure gas temperatures at the gasifier, cyclone filter, heat exchanger, and dried bed filter exits. During the process, Jatropha seed was converted into producer gas. The hot and dirty gas was cooled and cleaned by the cleaning unit.

Initially, some burning charcoal was placed on the grate of the gasifier. Biomass was then poured into the gasifier. The air blower was turned on to introduce air enabling incomplete combustion of the biomass. About five min later, gas was produced. It was then used to run the engine for the next 20 min. An orifice and U-tube manometer were employed to measure the gas flow rate.

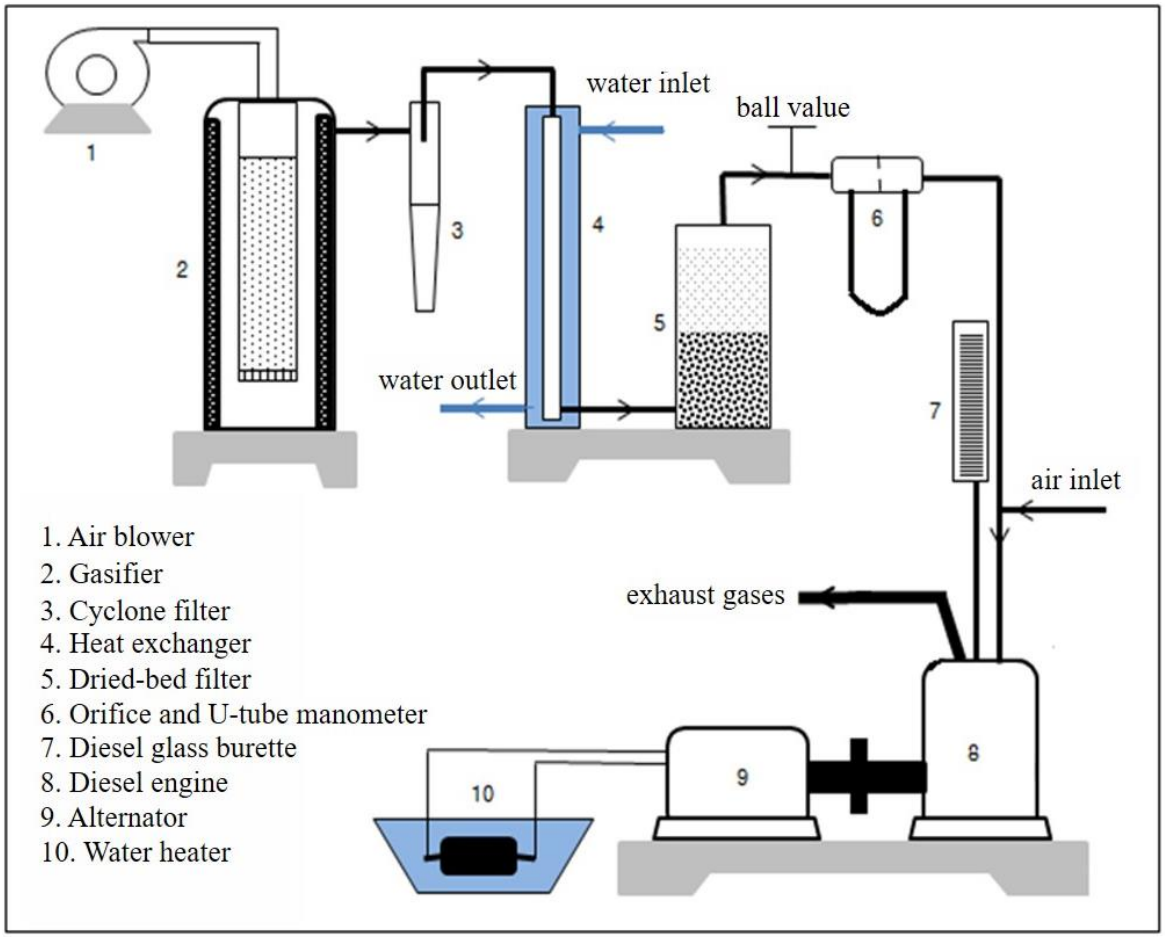

Figure 9 Schematic diagram of the designed gasifier-engine system

Table 5 Assumed and actual temperatures of producer gas at various crucial points

Position	At the gasifier outlet	At the heat exchanger outlet	At the engine inlet
Assumed	250 ℃	100 ℃	27 ℃
Actual	175 ℃	75 ℃	27 ℃

5. Results and observations

5. 1. Observations

The Jatropha seed was successfully gasified by the designed gasifier, and the producer gas was then used to run a diesel engine in a dual fuel mode. The maximum temperature of the gas at the gasifier exit was 175 ℃. The cyclone filter effectively collected the tar (see Figure 8, lower right) and cooled the gas to 75 ℃. After that, the shell-tube heat exchanger cooled the gas close to the ambient temperature using 5 ℃ cooling water. The observed and assumed temperatures are listed in Table 5. It is noteworthy that the assumed and actual temperatures at the engine inlet exactly matched.

The engine was successfully operated at a high speed of 3,000 rpm for three hours. The average biomass consumption rate was 5 kg/h, and the maximum gas production rate was up to 27 kg/h. A 20 kg/h gas flow replaced diesel fuel up to 49 % when the engine was operated at 70% of the full load. The diesel replacement rate would have been higher had the engine been operated at a medium engine speed. The power derating was 30% of the full engine load, which is higher than the assumed power derating of 20%. This could be explained that the assumed value was based on the previous study of medium engine speed, while the engine of this study was operated at a high speed of 3,000 rpm. Also, it was observed that the engine operation was stable and efficient at a high engine load with a gas flow rate of 10 kg/h on dual fuel mode. The poor combustion was noted at a high gas flow rate and high engine speed. The dual fuel engine should be operated at high engine load, but not at high engine speed and the maximum diesel replacement rate to maximize the electricity production per kilogram of diesel fuel.

Overall, the proposed heuristic concept in this paper makes a contribution to design a gasifier system that fits well the desired engine capacity based on basic theory and a heuristic concept, avoiding an oversize and cumbersome fabrication.

5.2 Engine performance and emission characteristics

Figure 10 illustrates the specific diesel consumption influenced by gas flow rate and engine load. Increases in gas flow rate and engine load had significant effects of reducing specific diesel consumption. This finding was also observed by [11]. The minimum specific diesel consumption was found with a 10-20 kg/h gas flow rate at a 2 kWe engine load.

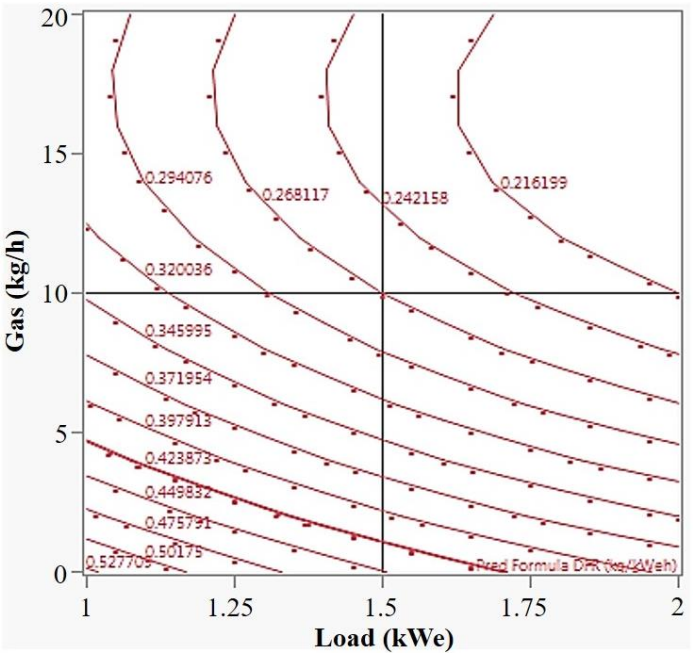

Figure 10 Specific diesel consumption (kg/kWeh)

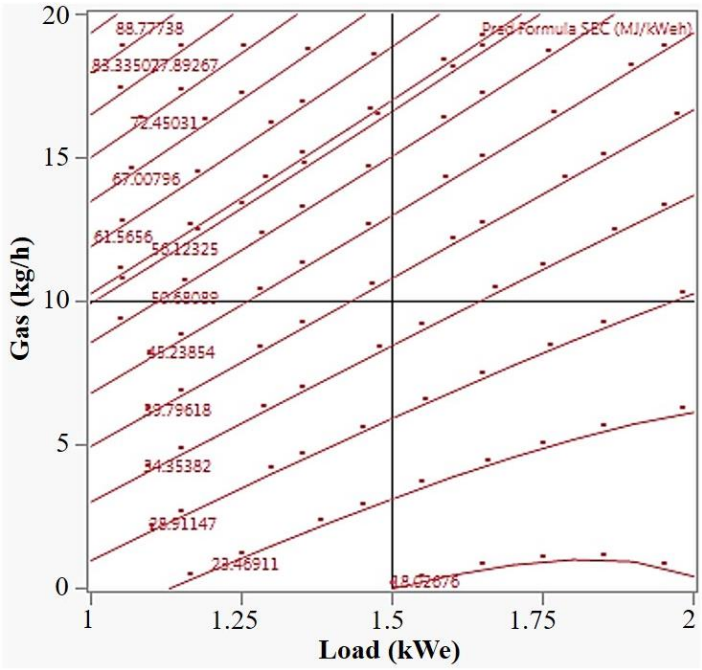

Figure 11 Specific energy consumption (MJ/kWeh)

Based on Figure 10, the dual fuel engine should be operated at a gas flow rate of 10 kg/h and high engine load because an increase in gas flow rate to more than 10 kg/h did not reduce the diesel consumption rate when the engine was operated at a high load. Another study also suggested that a dual fuel engine should be operated at a 10 kg/h gas flow rate and a high engine load to offset diesel consumption and the level of specific CO_2 emissions [11].

Figure 11 shows the specific energy consumption in terms of gas flow rate and engine load. An increase in gas flow rate was associated with higher energy consumption, but the specific energy consumption was noticeably reduced with an increased engine load. This was also reported by [11]. The dual fuel engine should be operated at high engine load to lessen energy consumption per kWe.

The specific HC and CO emissions are illustrated in Figure 12 and Figure 13, respectively. The presence of HC and CO emissions in exhaust gases implies incomplete combustion [2]. An increase in gas flow rate is associated with higher HC and CO emissions. However, lower specific HC and CO emissions were observed at higher engine loads in light of better combustion at higher loads. The same findings were reported in previous studies [5, 11-12].

The specific CO_2 emissions are illustrated in Figure 14. An amount of specific CO_2 emissions rose with an increase in gas flow rate due to the initial presence of CO_2 in the

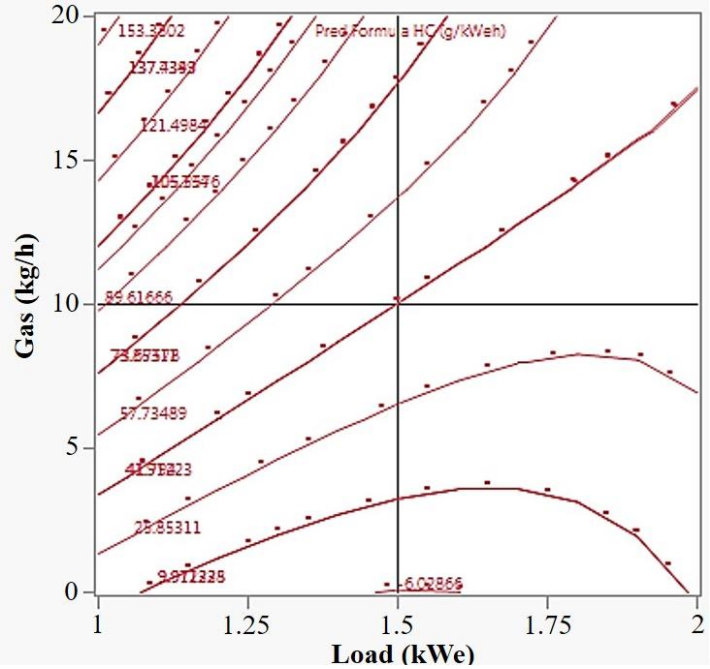

Figure 12 Specific HC emissions (g/kWeh)

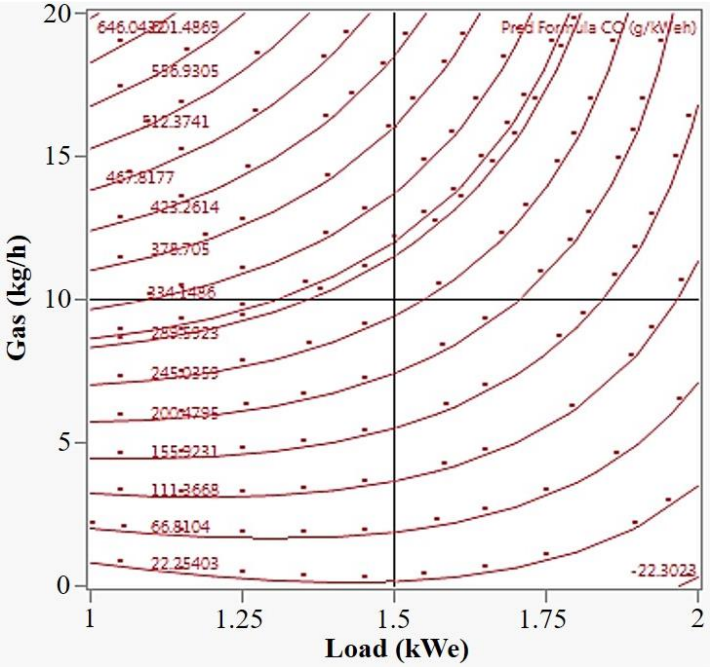

Figure 13 Specific CO emissions (g/kWeh)

producer gas [2]. A higher level of CO_2 emissions was associated with engine operation at a higher load due to more complete combustion. This was also observed by [11].

6. Conclusions and recommendations

This study intends to provide a heuristic concept to determine the dimensions of a downdraft gasifier and gas cleaning components for a pilot-scale diesel engine based on the basic theory of fluid dynamics and heat transfer. Beforehand, biomass feedstock, gasifier type, and an engine type are chosen to provide information for determining the dimensions of a gasifier, a cyclone filter, and a heat exchanger. After that, the gasifier's inner diameter is calculated based on the maximum gasification efficiency and thermal energy consumption of the gaseous fuel. Then, the cyclone filter's dimensions are determined using the ideal gas principle. Next, basic heat transfer theory and fluid dynamics are applied to design a shell-tube heat exchanger. A slight mass of small-sized charcoal pieces and a synthetic fiber filter are used to design a dried-bed filter to absorb the remaining tar and particles. In our study, Jatropha seed was chosen as the feedstock sample and a 5.7 kW diesel engine was coupled to the designed gasifier. The inner diameter of the designed gasifier was 150 mm. After ascertaining the

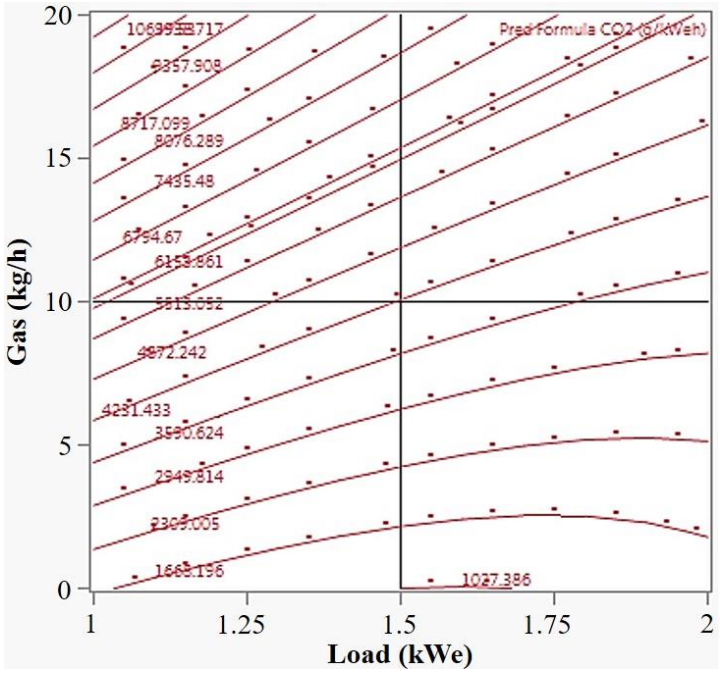

Figure 14 Specific CO_2 emissions (g/kWeh)

calculated dimensions, the gasifier was fabricated. The results highlighted that the fabricated gasifier can be used to convert biomass into a combustible gas, and the cleaning-cum-cooling unit can clean and cool the gas. The Jatropha-derived producer gas was used to run a diesel generator set in a dual gas-diesel mode. However, this mode is less efficient than the neat diesel mode. A 20 kg/h gas flow replaced diesel fuel by up to 49% when the engine was operated at 70% of the full engine load. The power derating was 30% and gasification efficiency was 77%. The maximum gas production rate was 27 kg/h. Based on the study of engine performance and emission characteristics, the dual fuel engine should be operated at a high engine load and a gas flow rate of 10 kg/h rather than at a maximum diesel replacement rate.

The proposed concept to determine the dimensions of the gasifier and the gas cleaning elements used the basic theory of the fluid dynamics and heat transfer. This is a reliable way to avoid an oversized and inefficient design. This approach is expected to minimize fabrication costs, improve biomass utilization, and reduce engine maintenance costs. The dual-fuel engine should not be operated at the maximum diesel replacement rate at high engine speeds.

A future study should focus on the environmental and energy benefits as well as the commercial feasibility of the gasifier-generator set using carbonaceous biomass to partially reduce diesel fuel consumption. Optimization of the gasifier's diameter and height using an experimental design approach (e.g., Response Surface Methodology) should be employed in future studies.

7. Acknowledgments

The results of this paper were funded by the Japan International Cooperation Agency (JICA) under the AUN/SEED-Net Project for a Master's Degree program at De La Salle University, Philippines.

8. References

[1] Basu P. Biomass gasification and pyrolysis-practical design and theory. London: Elsevier; 2010.

[2] Yaliwal VS, Banapurmath NR, Gireesh NM, Tewari PG. Production and utilization of renewable and sustainable gaseous fuel for power generation applications: a review of literature. Renew Sustain Energ Rev. 2014;34:608-27.

[3] Homdoung N, Tippayawong N, Dussadee N. Prediction of small spark ignited engine performance using producer gas as fuel. Case Stud Therm Eng. 2015;5:98-103.

[4] Tsiakmakis S, Mertzis D, Dimaratos A, Toumasatos Z, Samaras Z. Experimental study of combustion in a spark ignition engine operating with producer gas from various biomass feedstocks. Fuel. 2014;122:126-39.

[5] Sutheerasak E, Pirompugd W, Sanitjai S. Performance and emissions characteristics of a direct injection diesel engine from compressing producer gas in a dual fuel mode. Eng Appl Sci Res. 2018;45(1):47-55.

[6] Raheman H, Padhee D. Combustion characteristics of diesel engine using producer gas and blends of jatropha methyl ester with diesel in mixed fuel. Int J Renew Energ Dev. 2014;3(3):228-35.

[7] Singh R, Singh S, Pathak B. Investigations on operation of CI engine using producer gas and rice bran oil in mixed fuel mode. Renew Energ. 2007;32:1565-80.

[8] Banapurmath NR, Tewari PG. Comparative performance studies of a 4-stroke CI engine operated on dual fuel mode with producer gas and Honge oil and its methyl ester (HOME) with and without carburetor. Renew Energ. 2009;34:1009-15.

[9] Uma R, Kandpal T, Kishore V. Emission characteristics of an electricity generation system in diesel alone and dual fuel modes. Biomass Bioenerg. 2004;27:195-203.

[10] Martinez JD, Mahkamov K, Andrade RV, Lora EE. Syngas production in downdraft biomass gasifiers and

its application using internal combustion engines. Renew Energ. 2012;38:1-9.
[11] Rith M, Arbon N, Biona JBM. Optimization of diesel injection timing, producer gas flow rate, and engine load for the diesel engine operated on dual fuel mode at a high engine speed. Eng Appl Sci Res. 2019;46(3):192-99.
[12] Rith M, Biona JBM, Gitano-Briggs HW, Sok P, Gonzaga J, Arbon N, et al. Performance and emission characteristics of the genset fuelled with dual producer gas–diesel. DLSU Research Congress; 2016 Mar 7-9; Manila City, Philippines.
[13] Maiti S, Bapat P, Das P, Chosh PK. Feasibility study of jatropha shell gasification for captive power generation in biodiesel production process from whole dry fruits. Fuel. 2013;121:126-32.
[14] Shrivastava V, Jha AK, Wamankar AK, Murugan S. Performance and emission studies of a CI engine coupled with gasifier running in dual fuel mode. Procedia Eng. 2013;51:600-8.
[15] Dhole A, Yarasu R, Lata D. Investigations on the combustion duration and ignition delay period of a dual fuel diesel engine with hydrogen and producer gas as secondary fuels. Appl Therm Eng. 2016;107:524-32.
[16] Roy MM, Tomita E, Kawahara N, Harada Y, Sakane A. Performance and emission comparison of a supercharged dual-fuel engine fueled by producer gases with varying hydrogen content. Int J Hydrogen Energ. 2009;34:7811-22.
[17] Banapurmath NR, Tewari PG, Yaliwal VS, Kambalimath S, Basavarajappa YH. Combustion characteristics of a 4-stroke CI engine operated on Honge oil, Neem and Rice Bran oils when directly injected and dual fuelled with producer gas induction. Renew Energ. 2009;34:1877-84.
[18] KIPOR. Kipor power operation manual [Internet]. 2010 [Cited 2019 Sep 27]. Available from: https://www.maruagro.com/img/kcfinder/files/KD188F%20usuario-MANUAL%20DE%20USUARIO.pdf.
[19] Das D, Dash S, Ghosal M. Performance study of a diesel engine by using producer gas from selected agricultural residues on dual-fuel mode of diesel-cum-producer gas. World Renewable Energy Congress; 2011 May 8-13; Linkoping, Sweden.
[20] Ramadhas AS, Jayaraj S, Muraleedharan C. Dual fuel mode operation in diesel engines using renewable fuels: Rubber seed oil and coir-pith producer gas. Renew Energ. 2008;33:2077-83.
[21] Kreith F, Manglik R, Bohn M. Principles of heat transfer. 7th ed. Stamford: Global Engineering; 2011.
[22] Jain AK, Goss JR. Determination of reactor scaling factors for throatless rice husk gasifier. Biomass Bioenerg. 2000;18:249-56.
[23] Dogru M, Howarth CR, Akay G, Keskinler B, Malik AA. Gasification of hazelnut shells in a downdraft gasifier. Energy. 2002;27:415-27.
[24] Reed TB, Das A. Handbook of biomass downdraft gasifier engine systems. Washington: Government Printing Office; 1988.
[25] Patil K, Bhoi P, Huhnke R, Bellmer D. Biomass downdraft gasifier with internal cyclonic combustion chamber: design, construction, and experimental results. Bioresour Technol. 2011;102:6286-90.
[26] Olgun H, Ozdogan S, Yinesor G. Results with a bench scale downdraft biomass gasifier for agricultural and forestry residues. Biomass Bioenerg. 2011;35:572-80.
[27] Munson BR, Young DF, Okiishi TH, Huebsch WW. Fundamentals of fluid mechanics. 6th ed. New Jersey: John Wiley & Sons; 2009.
[28] Power N. Laminar vs Turbulent – Nusselt Number [Inernet]. 2019 [Cited 2019 Aug 04]. Available from: https://www.nuclear-power.net/nuclear-engineering/heat-transfer/convection-convective-heat-transfer/laminar-vs-turbulent-nusselt-number/.